

Article

Comparison of Various Analysis Methods Based on Heat Flowmeters and Infrared Thermography Measurements for the Evaluation of the In Situ Thermal Transmittance of Opaque Exterior Walls

Doo Sung Choi ¹ and Myeong Jin Ko ^{2,*} 

¹ Department of Building Equipment & Fire Protection System, Chungwoon University, Incheon 22100, Korea; trebelle@chungwoon.ac.kr

² Nabi Building Environment & Equipment Design Consultant Co., Ltd., Seoul 06226, Korea

* Correspondence: whistlemj@nate.com; Tel.: +82-2-6245-2504

Received: 11 June 2017; Accepted: 12 July 2017; Published: 18 July 2017

Abstract: There are several methods to obtain the in situ thermal transmittance value (U -value) of building envelopes from on-site data, including the three approaches of the progressive average method, average method considering the thermal storage effect, and dynamic method for deriving the U -value from heat flowmeter (HFM) measurements and the four methods with different formulas to analyze infrared thermography (IRT) measurement data. Since each of these methods considers different parameters and the non-steady characteristics of the heat transfer in building walls in their own way, discrepancies may occur among the obtained results. This study evaluates and compares the in situ U -values by using various methods of analyzing HFM and IRT measurement data. Further, by investigating buildings with similar materials and identical stratigraphies, but with different construction years, we analyze the discrepancy between the designed and measured values caused by material deterioration and evaluate the errors according to the analysis method. The percentage deviation between the U -values obtained by the three methods from the HFM data is found to be satisfactory, being within 10%. When compared with the results of the progressive average method, the deviations for the four different IRT-measurement-based methods vary greatly, being in the range of 6–43%.

Keywords: in situ thermal transmittance; heat flowmeter; infrared thermography; on-site measurement; opaque exterior wall

1. Introduction

Building energy consumption is currently increasing worldwide due to population increase and improvements in the quality of life. As a contributor to increasing energy consumption and the production of greenhouse gas emissions, the building sector is partly responsible for environmental pollution. Therefore, many countries have enacted regulations and laws aimed at increasing the energy performance of buildings. For example, some recent European directives encourage policy actions to reduce the energy requirement for heating and cooling by 20% by 2020 and 80% by 2050 compared to the energy requirement in 1990 [1]. In this regard, it is very important to estimate the actual energy performance of the building envelope.

The thermal transmittance value (U -value) of building walls is one of the key parameters utilized for the assessment of the energy sustainability of the entire building structure [2]. Therefore, construction and refurbishment of buildings is generally permitted based on the U -value established according to the minimum energy performance requirement and the local climate. However, the actual

U -value experimentally measured for buildings may differ significantly from the one estimated through theoretical calculation during the design phase. In both existing and new buildings, an inaccurate estimate of the U -value can provide misleading information on the building energy performance, which not only prevents the owner from establishing a reasonable energy consumption plan, but can also lead to economic losses via missing the renovation period and choosing inappropriate retrofitting activities. Therefore, it is important to investigate the in situ U -value of the building envelope through measurements.

Currently, the common measurement methods utilized to evaluate the in situ U -value of the building walls are the heat flowmeter (HFM) and infrared thermography (IRT) methods. The HFM method, regulated by ISO 9869-1 [3], is able to calculate the instantaneous and averaged U -value by measuring the heat flow through the wall and the temperature difference between indoors and outdoors. However, this method only affords a point measurement value, which can fail to detect imperfections, and thus, the estimated value may not accurately represent non-homogenous building elements [4]. Furthermore, in order to obtain reliable values, a minimum measurement interval of 72 h and minimum gradient of 10 °C between the indoor and outdoor temperatures are required. In the literature, some authors [5–10] have demonstrated that the experimental U -values obtained by the HFM method are often very different from the calculated ones due to thermal bridges, weather, ageing of the materials, and the types of sensors used and their partial adhesion to the wall. For example, Adhikari et al. [5] observed that the difference between the calculated and measured U -values varies considerably from 2% to 58%, depending on the materials of historical building walls. Asdrubali et al. [6] found that the measured and calculated U -values are not in perfect agreement and that the in situ U -value was up to 43% higher than the theoretical one. Cesaratto et al. [7] determined that the measurement location exerted strong influence on the evaluation accuracy of the U -value, and the maximum error varied up to 46% relative to the theoretical U -values.

The IRT method affords the spatially resolved temperature distribution of a wall surface based on the measurement of the distribution of the radiant thermal energy emitted from a target [11]. Therefore, this method has been widely applied in building diagnostics for qualitative evaluation to detect heat losses, air leakages, thermal bridges, sources of moisture, missing materials, and defects in insulation materials [12–16]. Furthermore, several researchers have recently studied the quantitative IRT method as an alternative approach to the in situ U -value measurement of the building envelope because it is both rapid and non-invasive [4,17–22].

As an example, Albatici and Tonelli [17] proposed the IRT method in order to acquire quantitative data of the actual U -values of the building envelope under a quasi-steady state condition and reported that the average U -value of the external wall as measured with the IRT method is 31% higher than the one measured with the HFM method. Further, they recommended the environmental conditions for a reliable measurement: avoidance of direct solar radiation, wind velocity below 1 m/s, a difference of at least 10–15 °C between the internal and external temperatures, with the room temperature at a uniform level of 20 °C at least 48 h before measurement. Albatici et al. [18] carried out long-term monitoring for the validation of the quantitative IRT method in an experimental building composed of five different wall constructions based on the procedure for a previously proposed IRT method [17]. They reported discrepancies of 9–40% between the IRT and HFM results and that the IRT method yields results with a good repeatability index for heavy walls compared with those for light walls and super-insulated walls. Fokaides and Kalogirou [19] reported that U -values measured by the IRT method are satisfactorily accurate in the range of 10% to 20% when compared with the theoretical values following the ISO 6946 standards [23] and in the range of 10% when compared with the HFM result. Through their sensitivity analysis, they also demonstrated that the ambient reflected temperature and thermal emissivity are the key parameters affecting the accuracy of IRT measurements. Dall'O' et al. [20] reported that the percentage absolute deviation between the theoretical and measured U -values is acceptable, being within 40–45% for solid-mass buildings; however, this deviation was high (more than 50%) for well-insulated walls. Nardi et al. [21,22] studied the quantitative IRT method for measuring the in situ U -values of the building envelope. For a well-insulated wall, they reported

that the percentage deviations of the in situ U -value measured by the IRT method with respect to calculations and the HFM method ranged from 16% to 28% and from 2% to 37%, respectively [21]. They also reported three case studies [22], and the differences between the IRT and HFM results ranged between 1% and 47% for the three cases. Danielski and Fröling [4] reported a discrepancy of 4% for small wall areas and 11% for large wall areas between the U -values of a massive wooden wall measured by both the IRT and HFM methods.

As described above, the HFM and IRT measurement methods are widely used to investigate the in situ U -value of building walls in operation. However, there are many ways to obtain the U -value from the on-site measurement data: three analysis methods including the progressive average method, average method considering the thermal storage effect, and dynamic method are available for deriving the U -value through HFM measurements, and four different procedures have been proposed for determining the U -value through IRT measurements. Although several such analysis methods have been reported thus far, many existing studies have used certain specific methods to obtain the U -values of buildings analyzed in their case studies. In assessing the U -value, these methods apply different parameters or analyze the non-steady characteristic of the heat transfer in building walls in their own ways, thus resulting in a discrepancy among the obtained results. Therefore, this study synthetically evaluates and compares the in situ U -value via the application of various analysis methods to HFM and IRT measurement data. Identifying the difference in the measurement results through various analysis methods can improve the reliability of the U -value evaluation, provide accurate information regarding the building wall, and help to increase the economic benefits gained by the building owner by enabling the choice of appropriate renovation period and retrofitting activities.

On the other hand, material deterioration decreases the building thermal performance, thereby yielding a discrepancy between the designed and measured U -values. Therefore, from on-site measurements on the exterior walls of six apartment houses with similar materials and identical stratigraphies but of different construction years, we also analyze the discrepancies in the results of in situ U -values according to various assessment methods. In addition, the methods for evaluating in situ U -value have not thus far been fully explored and related studies are still ongoing. Thus, the residential building typology with high insulation investigated in this study can aid in widening knowledge of the limits and strengths of the methods and broaden the areas of their practical application.

2. Evaluation Methods of U -Value

2.1. Calculation Method

The U -value can be calculated with the theoretical approach regulated by ISO 6946 [23] based on an electrical analogy and steady-state conditions. Once the opaque wall's stratigraphy and material properties are known, the U -value can be determined by the following equations:

$$R_{tot} = R_{si} + \sum_i \frac{d_i}{\lambda_i} + R_{se}, \quad (1)$$

$$U_{DESIGN} = \frac{1}{R_{tot}}, \quad (2)$$

here, U_{DESIGN} represents the thermal transmittance value evaluated by the calculation method ($W/m^2 \cdot K$); d_i the thickness of the i -th layer (m); λ_i its thermal conductivity ($W/m \cdot K$); R_{tot} the total wall thermal resistance ($m^2 \cdot K/W$); and R_{si} and R_{se} the interior and exterior surface resistances ($m^2 \cdot K/W$), respectively.

However, it is impossible to apply the calculation method when the thickness and conductivity of each wall layer are not known. In addition, the calculation method does not accurately represent the in situ U -value when considering a variety of factors such as incorrect estimations of material properties, differences between the ideal laboratory and actual environments, and workmanship [6].

2.2. Heat Flowmeter Method

Evaluations of the in situ U -value can be performed in accordance with ISO 9869-1 [3]. The HFM method determines the in situ U -value by measuring the heat flux through an element with a heat flowmeter, with the temperatures on both sides of the element under steady-state conditions. Since steady-state conditions are never encountered at a site, long-term measurements, corrections for the thermal storage effect, or the application of a dynamic analysis model have to be performed to compensate for these conditions. Therefore, three approaches, the progressive average method, average method including the storage effect, and dynamic analysis method, may be used for analysis of the HFM data.

The progressive average method assumes that the U -value can be obtained by dividing the mean density of the heat flow rate by the mean temperature difference, with the average being taken over a sufficiently long period of time that allows a good estimation of equivalent steady-state behavior [19,24]. An estimate of the U -value can be obtained as:

$$U_{PAM} = \frac{\sum_{j=1}^n q_j}{\sum_{j=1}^n (T_{i,j} - T_{e,j})}, \quad (3)$$

here, U_{PAM} represents the thermal transmittance value evaluated by the progressive average method ($W/m^2 \cdot K$); n the number of measurement data; $q_{i,j}$ the density of heat flow rate (W/m^2); and $T_{i,j}$ and $T_{e,j}$ the interior and exterior ambient temperatures (K), respectively.

Meanwhile, a more accurate acquisition of the in situ U -value is influenced not only by the thermal behavior of the wall under non-steady-state conditions, but also by the error of the measuring equipment. This is why we analyze the in situ U -value reflecting the uncertainty due to the measurement error of the temperature and heat flow in this study. For the evaluation of the in situ U -value, the overall uncertainty is calculated as the root mean square value of the deviations of each error case from the base case as determined from Equation (3) and the standard deviation of the U -value determined by using the moving average method as follows [25]:

$$\delta U_{ERROR,all} = \sqrt{(U_{PAM} - U_{ERROR,T_i})^2 + (U_{PAM} - U_{ERROR,T_e})^2 + (U_{PAM} - U_{ERROR,Q})^2 + (S_{U_{MAM}})^2}, \quad (4)$$

here, $\delta U_{ERROR,all}$ represents the overall uncertainty in the thermal transmittance evaluation; $U_{ERROR,Q}$, U_{ERROR,T_i} , and U_{ERROR,T_e} the thermal transmittances calculated by applying the sensor errors due to heat flow rate, interior, and exterior temperature measurements, respectively; and $S_{U_{MAM}}$ the standard deviation of the thermal transmittance determined by using the moving average method. In Equation (4), it is necessary to determine the U -value including the error of each measuring device. To illustrate an example, the U -value considering the sensor error of the interior temperature measurement is calculated as follows [25]:

$$U_{ERROR,T_i} = \frac{\sum_{j=1}^n q_j}{\sum_{j=1}^n (T_{i,j} + \delta T_{i,j} - T_{e,j})}, \quad (5)$$

where $\delta T_{i,j}$ denotes the interior temperature sensor error (K).

Since steady-state conditions do not occur in practice and most building structures have high resistance and high thermal mass, variations in interior or exterior temperatures lead to large fluctuations in the heat flow through the building wall. Therefore, the average method including the thermal storage effect corrects the measured heat flux and determines the corrected U -value as follows [3]:

$$U_{AMSE} = \frac{\sum_{j=1}^n q_j - (F_i \delta T_i + F_e \delta T_e) / \Delta t}{\sum_{j=1}^n (T_{i,j} - T_{e,j})}, \quad (6)$$

$$F_i = \sum_{k=1}^N C_k \left[\frac{R_{ek}}{R_{tot}} + \frac{R_k^2}{3R_{tot}^2} - \frac{R_{ik}R_{ek}}{R_{tot}^2} \right], \quad (7)$$

$$F_e = \sum_{k=1}^N C_k \left[\frac{R_k}{R_{tot}} \left\{ \frac{1}{6} + \frac{R_{ik} + R_{ek}}{3R_{tot}} \right\} + \frac{R_{ik}R_{ek}}{R_{tot}^2} \right], \quad (8)$$

where U_{AMSE} denotes the corrected thermal transmittance taking into account the storage effect ($W/m^2 \cdot K$); F_i and F_e the interior and exterior thermal mass factors, respectively; Δt the interval between readings (s); δT_i the difference between the interior average temperature over 24 h prior to reading j and interior average temperature over the first 24 h of the analysis period (K); and δT_e the difference between the exterior average temperature over 24 h prior to reading j and exterior average temperature averaged over the first 24 h of the analysis period (K); N the number of layers that make up the wall; C_k the thermal capacity of each layer ($J/m^2 \cdot K$); R_{tot} the total thermal resistance of the wall ($m^2 \cdot K/W$); R_k the thermal resistance of each layer ($m^2 \cdot K/W$); R_{ik} the sum of thermal resistances from the indoor environment to the $k - 1$ th layer ($m^2 \cdot K/W$); and R_{ek} the sum of thermal resistances from the $k + 1$ th layer to the outdoor environment ($m^2 \cdot K/W$).

As described above, a more accurate U -value can be obtained by increasing the measurement period in the progressive average method and by applying the corrected heat flux in the average method including the thermal storage effect. On the other hand, the dynamic analysis method obtains the steady-state properties of a building element by use of the heat equation based on measurements when large variations occur in the temperatures and heat flow rates, and the thermal transmittance is subsequently determined [3]. Since the dynamic method is a sophisticated method, it is usually implemented in dynamic simulation programs.

In this study, the dynamic method for evaluating measured data is implemented in the LORD [26] package (version 3.2, Olaf Gutschker, BTU Cottbus/Angewandte Physik, Germany), which is a software for the dynamic modeling and calculation of thermal systems involving simple components such as walls, windows, whole rooms, or more complicated systems. In the LORD software package, the values of the individual elements for thermal networks, such as conductances and capacitances, can be estimated using the measured temperatures and heat fluxes. Thus, when all parameters of the thermal system are identified, the thermal transmittance of the system can be calculated.

The accuracy of the U -value prediction using the software depends on the choice of the appropriate thermal network model based on the user's experience and knowledge [27]. Therefore, after reviewing several models with different numbers of nodes, the model with three nodes inside the wall was selected, as shown in Figure 1. Moreover, three nodes inside the wall are usually sufficient to model an opaque exterior wall in most cases [27]. Figure 1 shows the typical thermal network for a simple wall with four nodes that is considered in the present study.

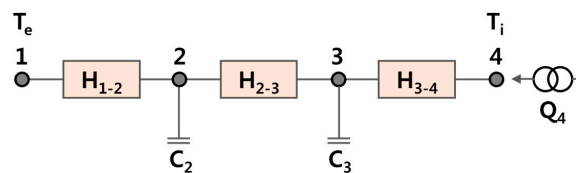


Figure 1. Thermal network model of measured wall comprising three conductances (H_{1-2} , H_{2-3} , and H_{3-4}) and two capacitances (C_2 and C_3).

This network model utilizes three conductances (H_{1-2} , H_{2-3} , and H_{3-4}), two capacitances (C_2 and C_3), and two boundary temperatures (T_e and T_i). The measured values include the ambient temperatures on both sides of the wall and the heat flux on the interior side. The heat flux on the interior surface is used for the definition of the objective function, which means that this heat flux must also be calculated and subsequently compared with the measured value [28]. The objective function that is described as the sum of the squares of the deviations between calculated and measured heat fluxes is minimized by the variation in parameters H_{1-2} , H_{2-3} , H_{3-4} , C_2 , and C_3 [28]. As a result of the parameter identification, the values of the three conductances and two capacitances are known, and the wall thermal transmittance $U_{DYNAMIC}$ can subsequently be calculated.

2.3. Infrared Thermography Method

The quantitative IRT method has been preferred over the HFM method for the calculation of on-site U -values because of its short measurement duration and ability to measure a wide area as opposed to the HFM method, which is time consuming and is more suitable for walls consisting of homogeneous material layers aligned perpendicular to the heat flow.

The first study for the evaluation of the U -value using the quantitative IRT method was performed by Madding [29], who suggested using the thermal resistance between the ambient air temperature and the surface temperature of the walls for calculating the heat transfer. Thus, the U -value is obtained as:

$$U_{IRT-Eq.(9)} = \frac{4\varepsilon\sigma T_m^3(T_{se} - T_{ref}) + h_c(T_{se} - T_e)}{T_i - T_e}, \quad (9)$$

where ε represents the thermal emissivity across the entire spectrum (-); σ the Stefan–Boltzmann constant ($5.67 \times 10^{-8} \text{ W/m}^2 \cdot \text{K}^4$); T_{se} the exterior wall surface temperature (K); T_{ref} the reflected temperature (K); T_m the mean temperature of the exterior wall surface temperature and the reflected temperature (K); and h_c the convective coefficient ($\text{W/m}^2 \cdot \text{K}$). The numerator in the equation represents the sum of the radiative and convective contributions whereas the denominator represents the difference between the interior and exterior air temperatures.

Fokaides and Kalogirou [19] proposed using the third power of the surface temperature T_{se} instead of the mean temperature T_m to calculate the U -value:

$$U_{IRT-Eq.(10)} = \frac{4\varepsilon\sigma T_{se}^3(T_{se} - T_{ref}) + h_c(T_{se} - T_e)}{T_i - T_e}, \quad (10)$$

here, a linearization of the Stefan-Boltzmann law is used to obtain the radiative heat transfer between the building surface and the surrounding. Fokaides and Kalogirou also performed a sensitivity analysis of the reflected temperature and reported that a deviation of 1°C in the measurement of the reflected temperature could cause errors of up to 10% in the calculation of the surface temperature and up to ~100% in the calculation of the thermal transmittance.

Dall'O' et al. [20] proposed the calculation of the U -value under the assumption that the heat flux between the environments separated by a wall can be expressed as the ratio of the heat flux calculated as a function of the exterior convective coefficient and the difference between the exterior surface and exterior air temperatures. The ratio of this heat flux to the difference between the interior and exterior air temperatures yields the U -value:

$$U_{IRT-Eq.(11)} = \frac{h_e(T_{se} - T_e)}{T_i - T_e} \text{ with } h_e = 5.8 + 3.8054v, \quad (11)$$

Dall'O' et al. found that the convective coefficient obtained from the Jurges equation [17,30] and the exterior heat transfer coefficient obtained from the American Society for Testing and Materials (ASTM) C 680 standard [31] based on the wind speed are similar for wind speeds of $<2 \text{ m/s}$. Therefore, in the interest of simplicity, the study used the Jurges equation for calculating the exterior heat transfer coefficient.

Recently, Albatici et al. [18] proposed the calculation of the U -value as the ratio of the sum of the radiative contribution using the Stefan-Boltzmann Law for a grey body and the convective contribution using the Jurges equation for a wind speed of $<5 \text{ m/s}$ to the difference between the interior and exterior temperatures:

$$U_{IRT-Eq.(12)} = \frac{\varepsilon_v\sigma(T_{se}^4 - T_e^4) + 3.8054v(T_{se} - T_e)}{T_i - T_e}, \quad (12)$$

here, ε_v denotes the wall emissivity in the wavelength range of the infrared camera and v is the wind speed (m/s).

Finally, Nardi et al. [32] compared the four different IRT methods proposed in the literature [18–20,29] by using a Guarded Hot Box (Butler Manufacturing, Kansas City, MO, USA), which allows the application of different operative conditions in a controlled environment.

3. In Situ Measurement of U -Value

3.1. Investigated Buildings

The measurement campaigns were conducted on the external walls of six apartment houses located in the central region of Korea from 31 January 2016 to 26 February 2016. The north-facing walls of each building were chosen for the test to minimize possible solar influence. The selection of these six buildings was made on the basis of different operational periods after construction in order to analyze the changes in thermal transmittances and the difference in results obtained by different analysis methods due to aging of the building components. The main features of the investigated buildings are listed in Table 1.

Table 1. Stratigraphies and thermophysical properties of the six cases examined, and the thermal transmittance values obtained by calculation method.

Cases	On-site Photo (Permission Year/ Construction Year)	Material Layer	d (mm)	λ (W/m·K)	R (m ² ·K/W)	U_{DESIGN} (W/m ² ·K)
Case 1	 (1985/1987)	Internal surface			0.110	0.431
		Gypsum board	10	0.180	0.056	
		Glass wool	70	0.035	2.000	
		Concrete	180	1.600	0.113	
		External surface			0.043	
Case 2	 (1993/1995)	Internal surface			0.110	0.429
		Gypsum board	10	0.180	0.056	
		Glass wool	70	0.035	2.000	
		Concrete	200	1.600	0.125	
		External surface			0.043	
Case 3	 (1999/2001)	Internal surface			0.110	0.418
		Gypsum board	10	0.180	0.056	
		Expanded polystyrene	70	0.034	2.059	
		Concrete	200	1.600	0.125	
		External surface			0.043	
Case 4	 (2007/2009)	Internal surface			0.110	0.312
		Gypsum board	12	0.180	0.067	
		Glass wool	100	0.035	2.857	
		Concrete	200	1.600	0.125	
		External surface			0.043	
Case 5	 (2009/2011)	Internal surface			0.110	0.280
		Gypsum board	12	0.180	0.067	
		Expanded polystyrene	100	0.031	3.226	
		Concrete	200	1.600	0.125	
		External surface			0.043	
Case 6	 (2012/2014)	Internal surface			0.110	0.269
		Gypsum board	10	0.180	0.056	
		Expanded polystyrene	105	0.031	3.387	
		Concrete	200	1.600	0.125	
		External surface			0.043	

In particular, the wall characteristics, construction year, and the calculated U_{DESIGN} -values according to ISO 6946 [23] are listed for each building. Information on the building materials for each building was obtained from the corresponding design documents. The test walls were made of gypsum board with a thickness of 10–12 mm, insulation with a thickness of 70–105 mm, and concrete with thickness of 180–200 mm. These configurations are representative of the construction solution techniques found in the Korean residential building stock. It can be observed that the thickness of the insulation and concrete increase with the strengthening of national energy regulations related to building insulation performance.

3.2. Measurement Procedure

Measurements of the in situ U -value utilizing the HFM method were performed in compliance with the ISO 9869-1 standard [3]: (i) the measurements have to be undertaken for at least 72 h with the difference between internal and external temperatures being equal or greater than 10 °C; (ii) the recording interval should be less than 0.5 h. For each of the six north-facing external walls, the temperature and heat flow measurements were conducted over 5 days between 31 January and 26 February 2016, and the data was logged in intervals of 10 min. During the measurement period, each dwelling was heated between average temperatures of 18.28 °C and 21.08 °C by means of the under-floor heating system depending on the homeowners' individual needs, thereby reflecting the living conditions. The test walls were exposed to the local outdoor weather conditions in the central region of Korea with average air temperature of -0.16 °C. Therefore, the difference between the indoor and outdoor average temperatures during the measurement was considerably greater than 10 °C, possibly resulting in a more precise result.

The in situ U -value of the test walls was measured by means of a heat flowmeter (Testo 435, Testo AG, Lenzkirch, Germany) with two temperature sensors. The heat flux sensor (Testo 0600 1635, Testo AG, Lenzkirch, Germany) had a sensitivity of $64.05 \mu\text{V}/(\text{W}/\text{m}^2)$, a working temperature range between -20 °C to $+50$ °C, and an expected accuracy of $\pm 5\%$. The indoor and outdoor air temperatures were measured by an in-built temperature sensor and by a temperature probe (Testo 0602 5792, Testo AG, Lenzkirch, Germany) with an accuracy of ± 0.3 °C, respectively.

A heat flux sensor was installed on the interior surface of the test wall of each dwelling after identifying the best position via an infrared camera. This infrared screening can aid in the positioning of the heat flow sensor at a suitable location to represent the thermal performance of the test wall without being disturbed by thermal anomalies such as thermal bridges. The external temperature sensor to measure the outdoor air temperature adjacent was applied to the north-facing wall away from direct solar radiation.

The measurements of the in situ U -value by means of the IRT method were carried out under the appropriate environmental conditions satisfying the various constraints indicated in the literature. In order to avoid direct solar radiation and the effects of thermal inertia and to achieve a quasi-steady-state condition, the measurements were conducted between 1:00 and 3:00 am, ensuring a difference of at least 10 °C between indoor and outdoor air temperatures and a wind speed less than 1 m/s. Although the measurements in this study were performed about 1–2 h earlier than the best period recommended in the previous researches [17,18], it was considered sufficient to minimize the influence of solar radiation. The wind speed was measured using a hot-wire anemometer (Testo 0635 1543, Testo AG, Lenzkirch, Germany) with a measurement range of 0 to 20 m/s and an accuracy of ± 0.03 m/s at a distance of 0.1 m from the test wall.

The reflected temperature and wall emissivity required to calculate the U -value of the test wall were measured using the infrared camera. First, the reflected temperature was measured in accordance with the ASTM E 1862-97 standard [33], using a highly reflective surface such as aluminum foil. With the infrared camera emissivity set to 1, the reflected temperature was obtained as the average temperature of the crumpled aluminum foil fixed on the surface of the test wall. As a second important parameter, the test wall emissivity, was measured in accordance with the ASTM E 1933-99 standard [34]

using a black adhesive tape with known emissivity. The wall spectral emissivity could be obtained by adjusting the emissivity of the infrared camera such that the temperature of the measured surface matched the temperature of the black tape. These measurements were conducted after a sufficient time interval to ensure that the aluminum foil and black tape reached the temperature of the test wall. The emissivity of the black adhesive tape (Temflex 1711, 3M, Taiwan) used in this study was 0.856 in the wavelength range of 5 to 20 μm , which was measured at a temperature of 40 $^{\circ}\text{C}$ using an FT-IR spectrometer (MIDAC, M2400-C, Boston, MA, USA).

The thermal images were acquired by a FLIR T620 infrared camera (FLIR systems, Portland, OR, USA) with a spectral range of 7.5 to 14 μm and resolution of 640 \times 480 pixels. The camera's noise equivalent temperature difference was lower than 0.04 $^{\circ}\text{C}$ at 30 $^{\circ}\text{C}$. The post-processing of the thermal images was performed with the FLIR Tools package (version 8.5, FLIR systems, Portland, OR, USA). As an example, Figure 2 shows the visible and infrared images utilized to evaluate the average surface temperature of the test wall.

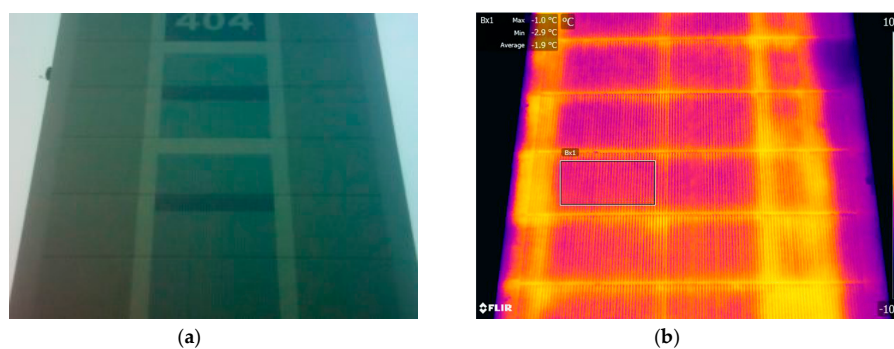


Figure 2. Images of the test wall for Case 1 (a) Visible; (b) infrared.

4. Results and Analysis

4.1. U -Value Obtained with Progressive Average Method

In situ U_{PAM} -values were estimated every 10 min based on the measurement campaign of 120 h for each case using the progressive average method as detailed in Section 2.2. Figure 3 shows the measured air temperatures and heat flux for the six cases.

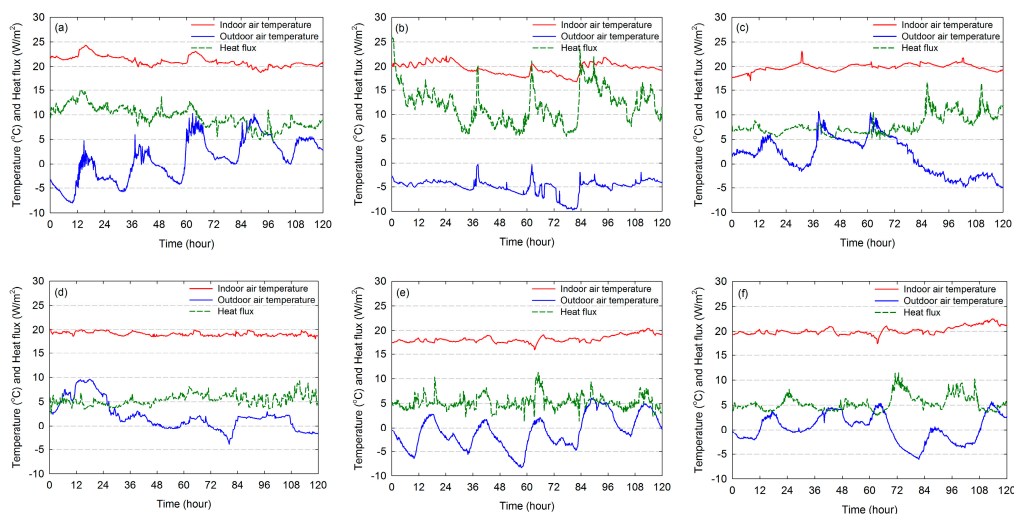


Figure 3. Measured heat flux at the indoor surface and indoor and outdoor air temperatures: (a) Case 1; (b) Case 2; (c) Case 3; (d) Case 4; (e) Case 5; (f) Case 6.

We note from the figure that the exterior air temperature for the whole monitoring period fluctuates in the range from $-9.75\text{ }^{\circ}\text{C}$ to $10.68\text{ }^{\circ}\text{C}$, while the interior air temperatures for each dwelling remain relatively constant around $20\text{ }^{\circ}\text{C}$ due to compensation by heating system. The average air temperature gradient throughout the monitoring period is lowest at $17.15\text{ }^{\circ}\text{C}$ for Case 4 and highest at $24.64\text{ }^{\circ}\text{C}$ for Case 2; these temperatures are considerably higher than the standard temperature condition, i.e., $10\text{ }^{\circ}\text{C}$ recommended by ISO 9869-1 [3]. The heat flux fluctuates according to the varying temperature difference across the wall. Under these non-steady conditions, the U_{PAM} -values and the U_{ERROR} -values calculated by applying the measurement uncertainty with a temperature sensor error of $0.5\text{ }^{\circ}\text{C}$ and the heat flow sensor error of 5% are shown in Figure 4 and listed in Table 2. From Figure 4, we note that the U_{PAM} -values for each case converge towards the corresponding asymptotical value although they are affected by measurement errors and weather conditions.

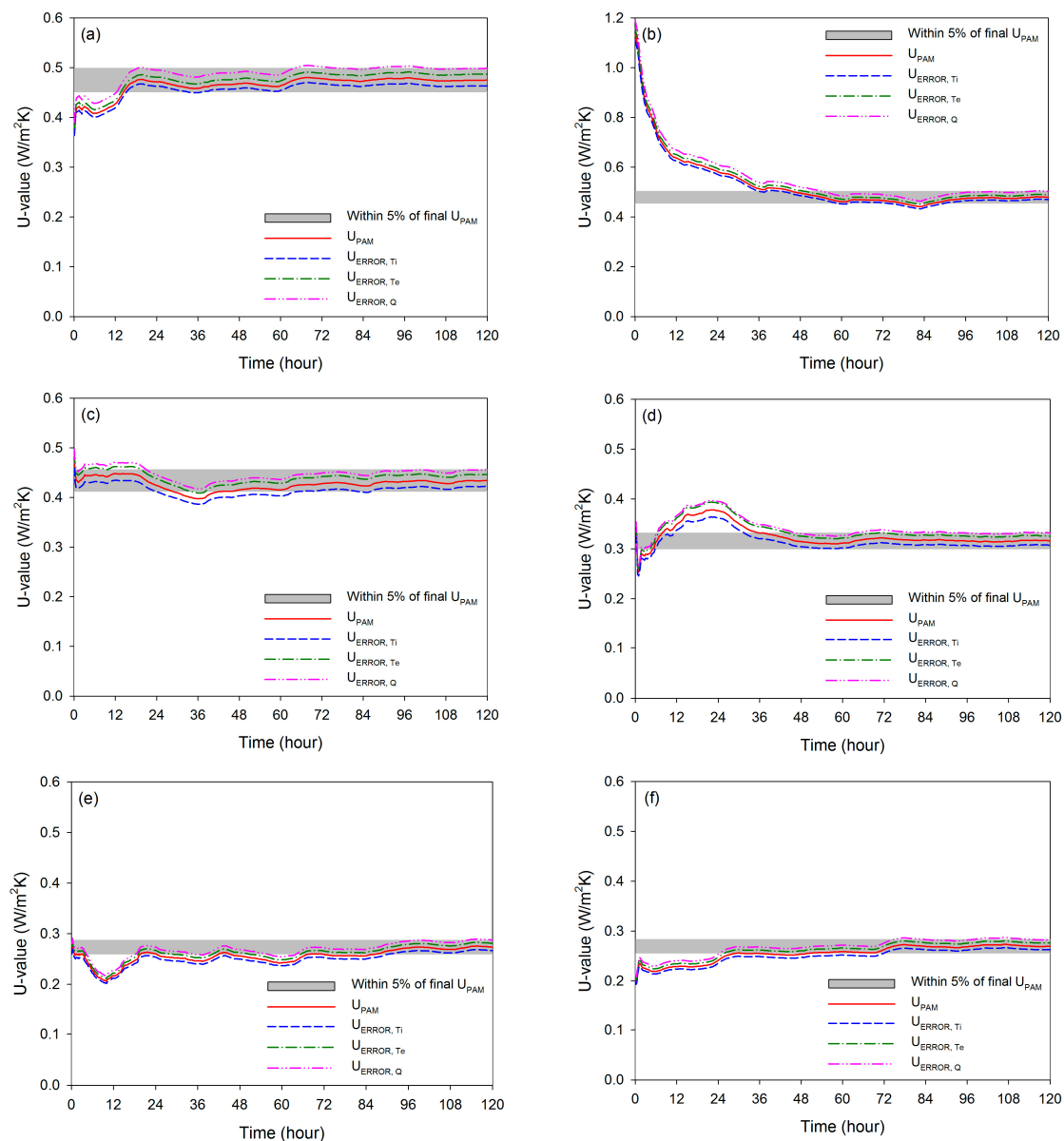


Figure 4. Evolution of in situ U -values analyzed by progressive average method and by progressive average method with application of measurement uncertainty: (a) Case 1; (b) Case 2; (c) Case 3; (d) Case 4; (e) Case 5; (f) Case 6.

However, these asymptotical values can be determined to be close to the actual U -values if the three following conditions are met [3]: (i) the test duration exceeds 72 h; (ii) the U -value obtained at the end of the test does not deviate by more than $\pm 5\%$ from the U -value obtained 24 h before; (iii) the U -value obtained by analyzing the data from the first time period corresponding to $\text{INT}(2 \times D_T/3)d$ does not deviate by more than $\pm 5\%$ from the U -values obtained from the data of the last time period of the same duration. The results show that the first and second conditions are satisfied in all six cases, but the third condition is not satisfied in Cases 5 and 6. Although, for Cases 5 and 6, the percentage deviations between the U -values calculated at 48 h and the corresponding final U -values calculated at 120 h are -6.38% and -5.80% , respectively (out of the range of $\pm 5\%$), it is clear that the percentage deviations are at an acceptable level, and the U -values converge towards the final U -values in the latter half of the measurement period. Therefore, the measurement period was not prolonged and the final U -values were analyzed as the in situ U -values by means of the progressive average method.

Meanwhile, the deviation width corresponding to $\pm 5\%$ of the final U_{PAM} -value for Case 1 is $0.048 \text{ W/m}^2\cdot\text{K}$, which is about 76.6% larger than the deviation width of $0.027 \text{ W/m}^2\cdot\text{K}$ for Case 6. In the non-steady state, the fluctuation of a less insulated wall is greater than one of a more insulated wall, but this fluctuation is largely offset by averaging the heat flux and temperature difference for the entire measurement period. Therefore, we found that a longer measurement time is required for a high-thermal-insulation wall.

Table 2 also lists the comparison between the U_{DESIGN} -values and the U_{PAM} -values together with their percentage deviations. The percentage deviations of the six cases range from -2.42% to 11.89% , which ranges are smaller than those reported in previous studies [5–7]. In particular, it can be clearly observed that the deviation between the calculated and measured U -values is smaller for recently constructed buildings. Meanwhile, the overall uncertainties of the in situ U -value measurements were the lowest at 6.98% in Case 1 and the highest at 14.75% in Case 2, and the maximum difference between the uncertainties of each case was up to 7.7%, which was not significant and occurred due to the high temperature difference across the test wall. These overall uncertainties in all the six cases lie within the range of 14% to 28% that is generally recommended by ISO 9869-1 [3].

4.2. U -Value Corrected by Application of Thermal Storage Effect

Figure 5 and Table 3 summarize the evolution of the U_{AMSE} -values corrected by the thermal storage effect and the comparison between the U_{DESIGN} -values and U_{AMSE} -values, respectively. In this study, the measured heat flux was corrected with respect to different analysis periods of 2 days, 3 days, and 4 days, which could provide corrected values of at least 1 day.

For all six cases, the U_{AMSE} -values and the U_{PAM} -values are very similar at the end of the measurement. From Figure 5, it can also be observed that the fluctuation of the U_{AMSE} -values is smaller than that of the U_{PAM} -values, and this effect becomes increasingly significant as the analysis period to apply the thermal storage effect increases. For example, in Case 2, the standard deviation of the U_{PAM} -value is 0.160 for 5 days, whereas the standard deviations of U_{AMSE} -values with different periods are 0.036 for 2 days, 0.015 for 3 days, and 0.006 for 4 days. Therefore, as per ISO 9869-1 [3], we found that the measurement period could be shortened when the in situ U -value is analyzed by applying this correction procedure.

In addition, from Table 3, similar to the cases analyzed in Section 4.1, we note that the percentage deviations between the U_{DESIGN} -values and the U_{AMSE} -values decrease for the recently constructed buildings. Therefore, from the field measurements, it can be concluded that the thermal performance of the building wall gradually deteriorates due to the material degradation resulting from the aging of building. It is necessary to make various efforts towards achieving energy efficiency of the existing building wall.

Table 2. Comparison of design U -values and in situ U -values analyzed by progressive average method, and overall uncertainties due to measuring-device error.

Cases	Construction Year	U_{DESIGN} (W/m ² ·K)	U_{PAM} (W/m ² ·K)	U_{PAM} Deviation Compared to U_{DESIGN} (%)	U_{PAM} Deviation during Test (%)		Uncertainty of U_{PAM}	
					24 h before End of Test	INT(2D _T /3)d before End of Test	$\delta U_{Err-all}$ (W/m ² ·K)	Overall Uncertainty (%)
Case 1	1987	0.431	0.475	10.25	0.86	−1.49	0.033	6.98
Case 2	1995	0.429	0.479	11.89	−0.94	3.25	0.071	14.75
Case 3	2001	0.418	0.434	3.92	−0.48	−4.34	0.037	8.43
Case 4	2009	0.312	0.316	1.15	−0.18	−0.49	0.025	7.85
Case 5	2011	0.280	0.273	−2.42	−0.48	−6.38	0.035	12.66
Case 6	2014	0.269	0.269	0.26	−0.27	−5.80	0.021	7.93

Table 3. Comparison between designed U -values and U -values corrected by applying the thermal storage effect.

Cases	Construction Year	U_{DESIGN} (W/m ² ·K)	U_{AMSE} for Different Analysis Periods (W/m ² ·K)			U_{AMSE} Deviation Compared with U_{DESIGN} (%)		
			$U_{AMSE-2days}$	$U_{AMSE-3days}$	$U_{AMSE-4days}$	$U_{AMSE-2days}$	$U_{AMSE-3days}$	$U_{AMSE-4days}$
Case 1	1987	0.431	0.467	0.479	0.474	8.44	11.26	10.02
Case 2	1995	0.429	0.496	0.467	0.453	15.70	8.92	5.79
Case 3	2001	0.418	0.443	0.450	0.440	5.99	7.72	5.25
Case 4	2009	0.312	0.309	0.317	0.307	−1.20	1.47	−1.65
Case 5	2011	0.280	0.295	0.282	0.275	5.50	0.65	−1.90
Case 6	2014	0.269	0.274	0.279	0.277	2.07	3.65	2.93

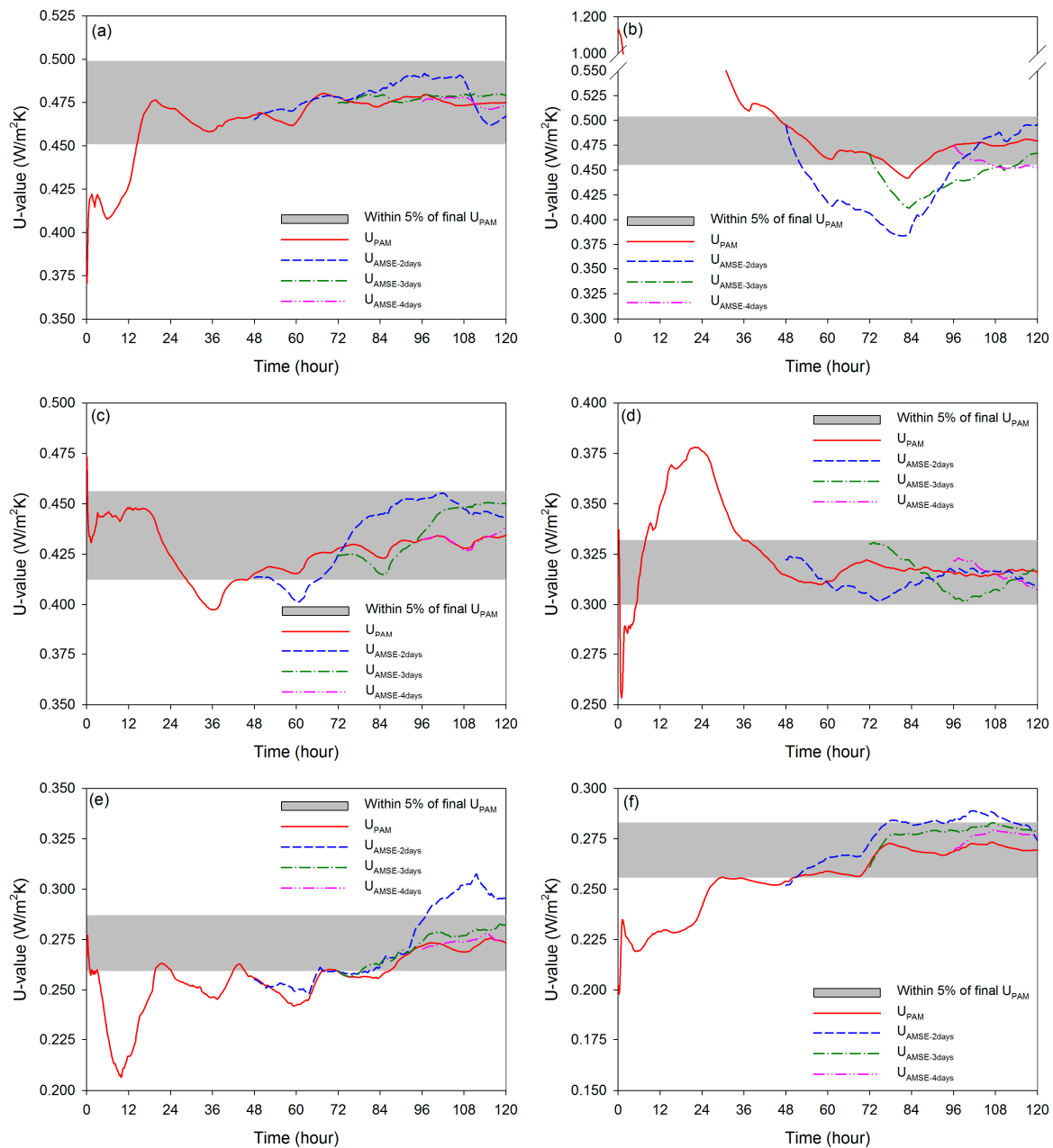


Figure 5. Evolution of U -values corrected by applying thermal storage effect: (a) Case 1; (b) Case 2; (c) Case 3; (d) Case 4; (e) Case 5; (f) Case 6.

4.3. U -Value Obtained with Dynamic Method

The dynamic method for evaluating in-situ measured data involves the use of the LORD software package [26–28,35,36], which allows the modeling and identification of thermal systems. In order to identify the parameters of the defined thermal network, such as thermal conductances and capacitances, the temperatures and heat flux at the boundary nodes of the network should be measured, and the temperature or the heat flux at one of these nodes needs to be selected as the output variable for comparison with the corresponding calculated parameter.

In this study, the measured heat flux progression on the interior surface was utilized for this purpose. Therefore, the software LORD could identify the parameters to minimize the sum of the squares of the deviations between the calculated and measured heat fluxes, and subsequently, the $U_{DYNAMIC}$ -values were derived. Figure 6 shows the measured and predicted heat fluxes together

with the residuals. It can be observed that the predicted heat fluxes are in good agreement with the measured heat fluxes. Figure 7 compares the $U_{DYNAMIC}$ -values, U_{DESIGN} -values, and U_{PAM} -values together with their percentage deviations. From the deviation observed between the $U_{DYNAMIC}$ and U_{PAM} values shown in Figure 7b, we note that in all cases, the deviations are less than 3% regardless of building aging. Therefore, it can be concluded that the dynamic method can determine the in situ U -value to a reasonable level of accuracy. In addition, the $U_{DYNAMIC}$ -values were found to be higher by 10.38% for Case 2 (building constructed in 1995 and higher by 1.20% for Case 6 (building constructed in 2014) in comparison with the corresponding U_{DESIGN} -values. These results are consistent with the fact that the mismatch between the measured and calculated U -values is smaller for recent buildings, as analyzed previously.

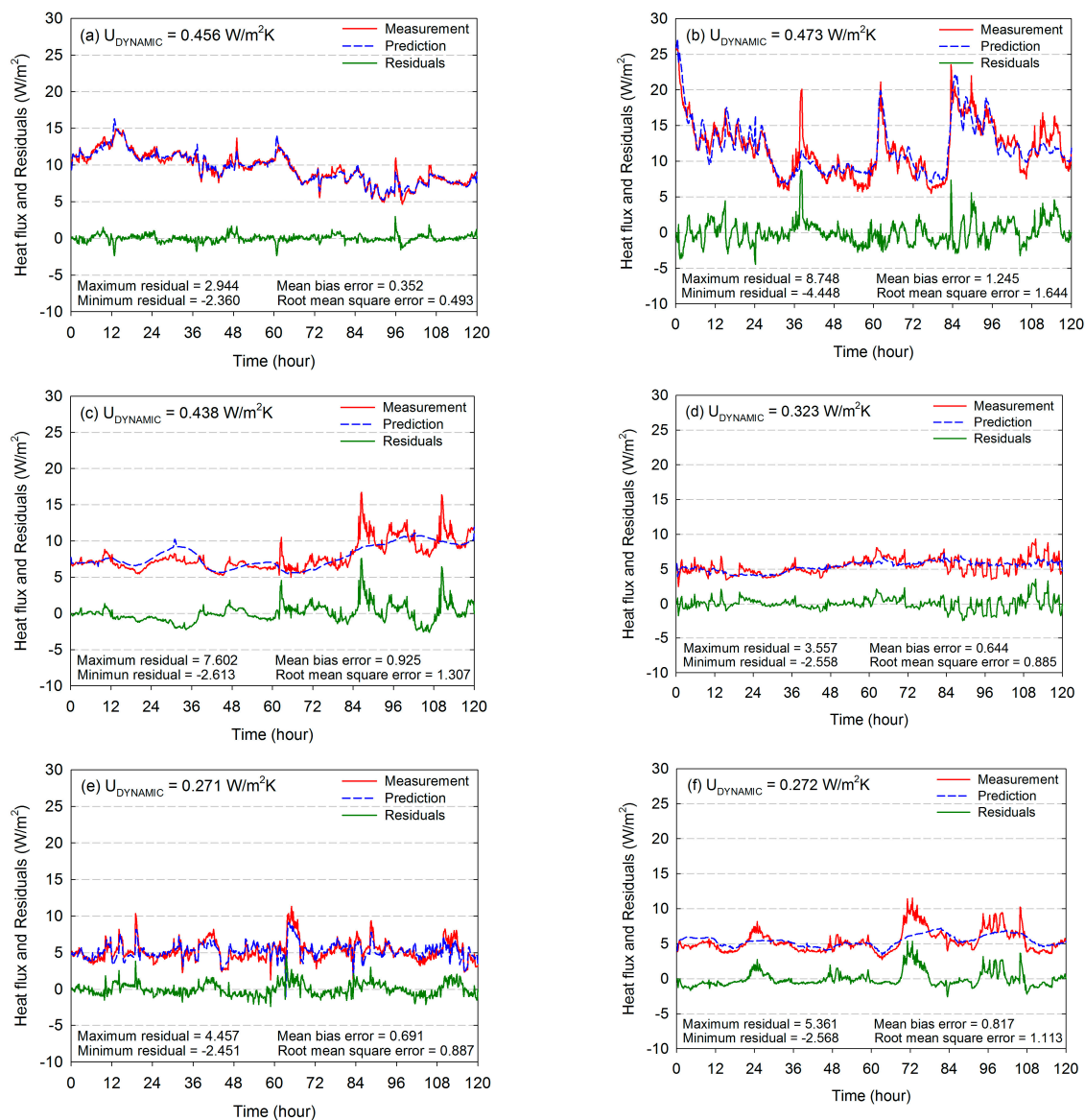


Figure 6. Comparison between measured and predicted heat fluxes: (a) Case 1; (b) Case 2; (c) Case 3; (d) Case 4; (e) Case 5; (f) Case 6.

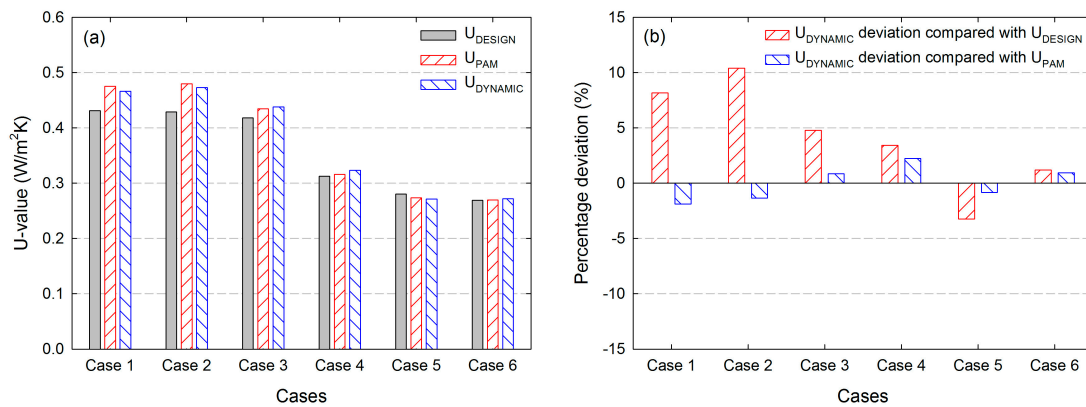


Figure 7. (a) U-values; (b) their percentage deviations estimated by calculation method, progressive average method, and dynamic method.

4.4. U-Value Obtained with Infrared Thermography Method

In this section, we examine the U_{IRT} -values obtained with the IRT method with the four different equations described in Section 2.3. These results are compared with the corresponding U_{DESIGN} -values. In Equations (9) and (10), the convective coefficient h_c is given by $3.8054 \times v_e$ and the wall emissivity ϵ_v in the wavelength range of the infrared camera is used instead of the emissivity across the entire spectrum. Table 4 lists the U_{IRT} -values calculated using Equations (9)–(12) together with the parameters required for the equations. The infrared thermographic surveys were performed between 1:00 and 3:00 am on days with an overcast sky in order to minimize the influence of solar radiation and radiative heat losses to the sky [17,18]. From Table 4, it can be inferred that the local wind speed in the vicinity of the test building wall was less than 0.2 m/s and the difference between indoor and outdoor air temperatures was greater than $\sim 20^\circ\text{C}$ during the survey. It is necessary that these conditions be satisfied in order to obtain accurate results and minimize errors arising from any instability.

Figure 8a shows the U_{IRT} -values determined through the IRT method; we note that the U_{IRT} -values differ according to the four different equations. In all the cases investigated, $U_{IRT-Eq.(9)}$ -values and $U_{IRT-Eq.(10)}$ -values estimated by Equations (9) and (10), respectively, are very similar because of the similarity of the equations. The $U_{IRT-Eq.(11)}$ -values calculated via Equation (11) do not show a large deviation from the $U_{IRT-Eq.(9)}$ -values and $U_{IRT-Eq.(10)}$ -values. On the other hand, the $U_{IRT-Eq.(12)}$ -values calculated with Equation (12) are $\sim 15\%$ to 30% less than $U_{IRT-Eq.(9)}$ -values and $U_{IRT-Eq.(10)}$ -values because of the reduced radiative contribution to the overall heat transfer due to the reflected temperature being lower than the outside air temperature.

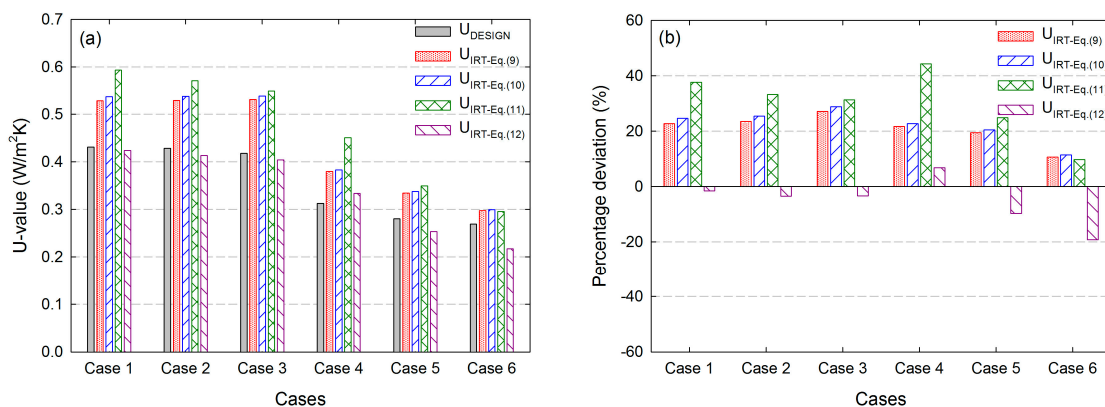


Figure 8. (a) U-values; (b) their percentage deviations estimated by calculation method and infrared thermography method.

Table 4. *U*-values obtained through infrared thermography method with four different equations together with required parameters.

Cases	Construction Year	U_{DESIGN} (W/m ² ·K)	T_{se} (°C)	T_e (°C)	T_i (°C)	T_{ref} (°C)	T_m (°C)	ε (-)	V_e (m/s)	U_{IRT} (W/m ² ·K)			
										Equation (9)	Equation (10)	Equation (11)	Equation (12)
Case 1	1987	0.431	-2.00	-4.50	21.87	-5.20	-3.55	0.90	0.12	0.529	0.537	0.593	0.424
Case 2	1995	0.429	-1.90	-4.25	21.66	-5.00	-3.48	0.91	0.13	0.529	0.538	0.571	0.414
Case 3	2001	0.418	0.80	-1.14	20.30	-1.80	-0.51	0.91	0.07	0.531	0.539	0.549	0.404
Case 4	2009	0.312	0.60	-0.78	18.62	-1.00	-0.25	0.90	0.14	0.380	0.383	0.450	0.334
Case 5	2011	0.280	-1.90	-3.08	17.78	-3.50	-2.76	0.91	0.10	0.334	0.337	0.350	0.253
Case 6	2014	0.269	-0.70	-1.68	19.61	-2.10	-1.42	0.90	0.16	0.297	0.299	0.295	0.217

Since these four procedures use parameters such as the wall surface temperature, reflected temperature, wall emissivity, and wind speed acquired by instantaneous measurements, some errors arising by not considering the thermal storage effect of the wall may occur. In order to quickly as well as accurately evaluate the in situ U -value using the quantitative IRT method, further studies are necessary to analysis the influence of these parameters on the results.

The percentage deviations with respect to the U_{DESIGN} -values are shown in Figure 8b. The U_{IRT} -values calculated with Equations (9)–(11) are larger than the corresponding U_{DESIGN} -values, while the $U_{IRT-Eq.(12)}$ -values calculated by Equation (12) are similar to or smaller than the corresponding U_{DESIGN} -values. The percentage absolute deviations of the U_{IRT} -values obtained by IRT method are generally within about 30% of the U_{DESIGN} -values, which is considered an acceptable level of accuracy when considering the results reported in previous studies [17–22].

4.5. Comparison of Different U -Value Evaluation Methods

Thus far, the results estimated by various evaluation methods such as the calculation method, progressive average method, average method with application of the thermal storage effect, dynamic method, and infrared thermography method have been individually analyzed in each corresponding section. In this section, the U -values obtained by these various methods are synthetically compared and evaluated for the six investigated cases with similar materials and identical stratigraphies but with different permission and construction years.

As in most countries in the world, the Korean government has been continuously enhancing the thermal performance of building facades by framing and improving regulations and laws. In terms of figures, the limits of the U -value for vertical opaque walls for the central region of Korea was maintained at $0.467 \text{ W/m}^2\cdot\text{K}$ until December 2000, but was reduced to $0.350 \text{ W/m}^2\cdot\text{K}$ in January 2001 and then further reduced to $0.270 \text{ W/m}^2\cdot\text{K}$ in November 2011. From Figure 9, it can be clearly observed that the U -values obtained from on-site measurements for the walls constructed long ago are higher than the corresponding design U -values. Based on the U_{PAM} -values obtained by the progressive average method, which is widely used as a reference method, the mean U_{PAM} -values corresponding to Cases 1 to 3 (buildings constructed before 2001) were about $0.177 \text{ W/m}^2\cdot\text{K}$ (61.7%) higher than the corresponding ones of Cases 4 to 6 (buildings constructed after 2009). Even the U_{PAM} -values of Case 1 and Case 2 exceed the legal limit at the time of construction and are 75.9% and 77.6% higher than the current one, respectively. Therefore, it can be argued that the in situ measurements should be continually performed in order to obtain information on the degradation of thermal performance and to plan the energy refurbishment of the existing building.

Unlike the other five cases, the U_{DESIGN} -value of Case 6 (building constructed in 2014) barely meets the legal standards. In order to satisfy the legal limit by a wide margin, we generally require thicker insulation materials, which leads to reduction in the effective floor area of the building and increase in the construction cost. Although further investigations on recently constructed buildings are needed, it is believed that the construction companies have recently built buildings with a level that barely meets the stricter standards. Therefore, these buildings, such as the one in Case 6, are expected to show a rapid deterioration in thermal performance in the future; further in situ thermal transmittance evaluations may be required.

From Figure 10, we note that when compared with the U_{PAM} -values obtained by the progressive average method, the percentage absolute deviations of the U_{AMSE} -values for the average method considering the thermal storage effect and the $U_{DYNAMIC}$ -value for the dynamic method are found to be fairly accurate, being within 10%. Therefore, these two methods can be utilized for short measurement periods although the difference between indoor and outdoor air temperatures should be equal to or greater than $10 \text{ }^\circ\text{C}$. On the other hand, the percentage absolute deviations between the U_{PAM} -values for the HFM method and U_{IRT} -values for the IRT method are in the range of 6–43% for the six cases investigated here. These relatively large deviations are due to differences in the measurement methods. While the progressive average method, average method considering the

thermal storage effect, and dynamic method ensure steady-state conditions and consider the storage effect caused by thermal mass in each specific way from the measurement period of at least 72 h, the IRT method that involves instantaneous measurements cannot take into account the effects of thermal inertia and the heat capacity of the wall. We believe that more extensive studies are required on improving the accuracy of in situ thermal transmittance evaluation using the IRT method.

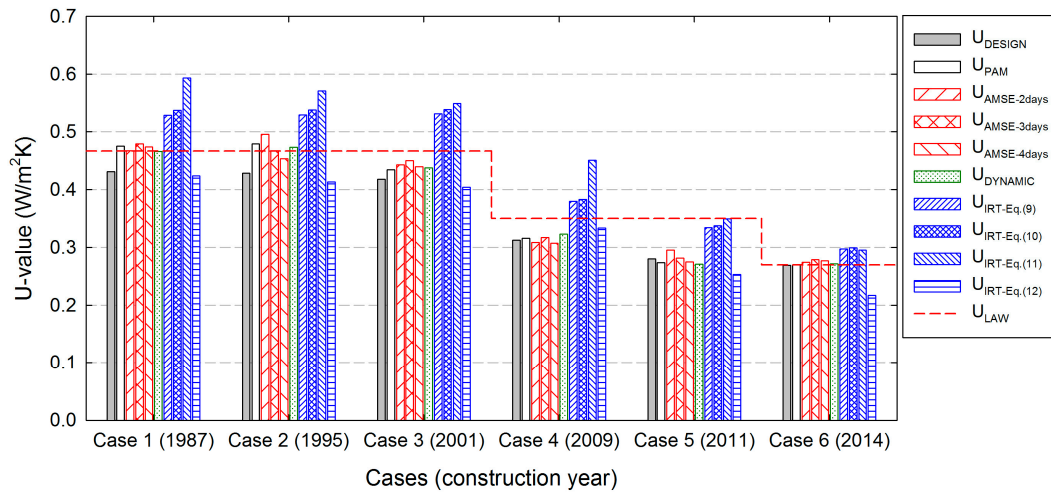


Figure 9. *U*-values obtained by calculation method, progressive average method, average method with application of thermal storage effect, dynamic method, and infrared thermography method for six investigated cases with different construction years.

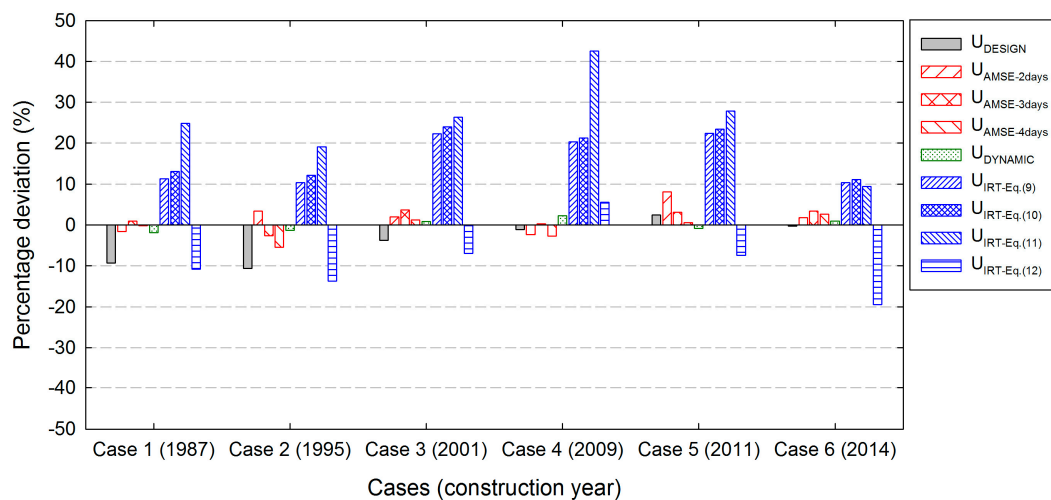


Figure 10. Percentage deviations among the *U*-values obtained by calculation method, average method considering the thermal storage effect, dynamic method, and infrared thermography method compared with one obtained by progressive average method.

5. Conclusions

In this study, after a presenting a brief review on the various methods that may be used for evaluating in situ *U*-value of an external building wall by HFM and IRT measurements, we compared the results of these methods as well as the design *U*-values obtained by the calculation method, normalized by ISO 6946. In order to analyze the discrepancy between the designed and measured *U*-values arising from material deterioration and errors of the analysis method, we selected six residential buildings with similar materials and identical stratigraphies but with different construction years. For each of the six north-facing external walls, HFM measurements were conducted in winter

over five days with an average temperature difference of at least 17 °C between the indoor and outdoor environments, and the data were acquired every 10 min. In order to obtain the correct U -value of the test wall under quasi-steady-state conditions, IRT measurements were carried out between 1:00 and 3:00 a.m., with a temperature difference of at least 20 °C across the test walls and a wind speed <0.2 m/s.

Our results show that for the U -values obtained with the progressive average method, the older is the building, the higher is discrepancy between the measured and designed U -values. For example, the in situ U -value of a test wall (Case 1) constructed 30 years ago not only exceeds the legal limit at that time but is also about 76% higher than the current one. This indicates that on-site measurements for evaluating in situ U -value should be continually performed in order to acquire information on the degradation of thermal performance and to plan the energy refurbishment of the existing building.

When compared with the U -values obtained by the progressive average method, the percentage absolute deviations of the U -values for the average method considering the thermal storage effect and the U -values for the dynamic method are found to be satisfactorily accurate, being within 10%. Therefore, it is considered that these methods may shorten the on-site measurement period. However, further studies are needed on the extent to which these two methods can shorten the measurement period and which environmental conditions should be met.

On the other hand, the percentage absolute deviation between the U -values obtained by the progressive average method and the four different formulas of the IRT method are found to be in the range of 6% to 43%. These relatively large deviations are considered to be due to the fact that different parameters are used in the equations and that thermal storage effect is not reflected. Therefore, our results indicate that more extensive researches are needed to improve the accuracy of the in situ thermal transmittance evaluation using the infrared thermography method. In particular, it is necessary to fully characterize the influence of various parameters on the obtained results through continuous infrared thermographic survey over a long period in a controlled laboratory environment as well as in an unpredictable actual environment.

Acknowledgments: This research was supported by a grant (17CTAP-C130211-01) from Technology Advancement Research Program (TARP) funded by Ministry of Land, Infrastructure and Transport of Korean government.

Author Contributions: All authors performed the measurement and wrote the paper together.

Conflicts of Interest: The authors declare no conflict of interest.

Nomenclature

C_k	Thermal capacity of each layer, J/m ² ·K
d	Material thickness, mm
F_e	Exterior thermal mass correction factor, J/m ² ·K
F_i	Interior thermal mass correction factor, J/m ² ·K
h_c	Convective coefficient, W/m ² ·K
n	The number of measurement data
N	The number of layers that make up the wall
$q_{i,j}$	Heat flux, W/m ²
R_{ik}	Sum of thermal resistances from the indoor environment to the $k - 1$ th layer, m ² ·K/W
R_{ek}	Sum of thermal resistances from the $k + 1$ th layer to the outdoor environment, m ² ·K/W
R_k	Thermal resistance of each layer, m ² ·K/W
R_{se}	Exterior surface resistance, m ² ·K/W
R_{si}	Interior surface resistance, m ² ·K/W
R_{tot}	Total thermal resistance of the wall, m ² ·K/W
$S_{U_{MAM}}$	Standard deviation of the thermal transmittance determined by the moving average method
$T_{e,j}$	Exterior ambient temperature, K
$T_{i,j}$	Interior ambient temperature, K
T_m	Mean temperature between the exterior wall surface temperature and the reflected temperature, K
T_{ref}	Reflected temperature, K
T_{se}	Exterior wall surface temperature, K
U_{AMSE}	Corrected thermal transmittance value taking into account the storage effect, W/m ² ·K
U_{DESIGN}	Thermal transmittance evaluated by the calculation method, W/m ² ·K

$U_{DYNAMIC}$	Thermal transmittance evaluated by the dynamic method, $W/m^2 \cdot K$
$U_{ERROR,Q}$	Thermal transmittance calculated by applying the heat flux sensor error, $W/m^2 \cdot K$
U_{ERROR,T_i}	Thermal transmittance calculated by applying the interior temperature sensor error, $W/m^2 \cdot K$
U_{ERROR,T_e}	Thermal transmittance calculated by applying the exterior temperature sensor error, $W/m^2 \cdot K$
U_{IRT}	Thermal transmittance evaluated by the infrared thermography method, $W/m^2 \cdot K$
U_{PAM}	Thermal transmittance evaluated by the progressive average method, $W/m^2 \cdot K$
v	Wind speed, m/s
δT_e	Difference between interior average temperature over 24 h prior to reading j and interior average temperature over the first 24 h of the analysis period, K
δT_i	Difference between exterior average temperature over 24 h prior to reading j and exterior average temperature over the first 24 h of the analysis period, K
$\delta T_{i,j}$	Interior temperature sensor error, K
$\delta U_{ERROR,all}$	Overall uncertainty in the thermal transmittance evaluation, $W/m^2 \cdot K$
ϵ	Thermal emissivity across the entire spectrum
ϵ_v	Thermal emissivity in the wavelength range of the infrared camera
λ_i	Thermal conductivity, $W/m \cdot K$
σ	Stefan-Boltzmann constant
Δt	Interval between readings, s

References

- Nardi, I.; Paoletti, D.; Ambrosini, D.; Rubeis, T.D.; Sfarra, S. Validation of quantitative IR thermography for estimating the U-value by a hot box apparatus. In Proceedings of the 33th UIT (Italian Union of Thermo-Fluid-Dynamics) Heat Transfer Conference, L'Aquila, Italy, 22–24 June 2015.
- Albatici, R.; Passerini, F.; Tonelli, A.M.; Gialanella, S. Assessment of the thermal emissivity value of building materials using an infrared thermovision technique emissometer. *Energy Build.* **2013**, *66*, 33–40. [CrossRef]
- ISO 9869-1:2014. Building Elements—In-Situ Measurement of Thermal Resistance and Thermal Transmittance—Part 1: Heat Flow Meter Method. Available online: <https://www.iso.org/standard/59697.html> (accessed on 13 July 2017).
- Danielski, I.; Fröling, M. Diagnosis of buildings' thermal performance—A quantitative method using thermography under non-steady state heat flow. *Energy Procedia* **2015**, *83*, 320–329. [CrossRef]
- Adhikari, R.S.; Lucchi, E.; Pracchi, V. Experimental measurements on thermal transmittance of the opaque vertical walls in the historical buildings. In Proceedings of the 28th International PLEA Conference on Sustainable Architecture + Urban Design, Lima, Peru, 7–9 November 2012.
- Asdrubali, F.; D'Alessandro, F.; Baldinelli, G.; Bianchi, F. Evaluating in situ thermal transmittance of green buildings masonries—A case study. *Case Stud. Constr. Mater.* **2014**, *1*, 53–59. [CrossRef]
- Cesaratto, P.G.; Carli, M.D. A measuring campaign of thermal conductance in situ and possible impacts on net energy demand in buildings. *Energy Build.* **2013**, *59*, 29–36. [CrossRef]
- Meng, X.; Yan, B.; Gao, Y.; Wang, J.; Zhang, W.; Long, E. Factors affecting the in situ measurement accuracy of the wall heat transfer coefficient using the heat flow meter method. *Energy Build.* **2015**, *86*, 754–765. [CrossRef]
- Peng, C.; Wu, Z. In situ measuring and evaluating the thermal resistance of building construction. *Energy Build.* **2008**, *40*, 2076–2082. [CrossRef]
- Evangelisti, L.; Guattari, C.; Gori, P.; Vollaro, R.D.L. In situ thermal transmittance measurements for investigating differences between wall models and actual building performance. *Sustainability* **2015**, *7*, 10388–10398. [CrossRef]
- Kylili, A.; Focaides, P.A.; Christou, P.; Kalogirou, S.A. Infrared thermography (IRT) applications for building diagnostics: A review. *Appl. Energy* **2014**, *134*, 531–549. [CrossRef]
- Haralambopoulos, D.A.; Paparsenos, G.F. Assessing the thermal insulation of old buildings—The need for in situ spot measurements of thermal resistance and planar infrared thermography. *Energy Convers. Manag.* **1998**, *39*, 65–79. [CrossRef]
- Balaras, C.A.; Argiriou, A.A. Infrared thermography for building diagnostics. *Energy Build.* **2002**, *34*, 171–183. [CrossRef]
- Ocana, S.M.; Guerrero, I.C.; Requena, I.G. Thermographic survey of two rural buildings in Spain. *Energy Build.* **2004**, *36*, 515–523. [CrossRef]

15. Kalamees, T. Air tightness and air leakages of new lightweight single-family detached houses in Estonia. *Build. Environ.* **2007**, *42*, 2369–2377. [[CrossRef](#)]
16. Taylor, T.; Counsell, J.; Gill, S. Energy efficiency is more than skin deep: Improving construction quality control in new-build housing using thermography. *Energy Build.* **2013**, *66*, 222–231. [[CrossRef](#)]
17. Albatici, R.; Tonelli, A.M. Infrared thermovision technique for the assessment of the thermal transmittance value of opaque building elements on site. *Energy Build.* **2010**, *42*, 2177–2183. [[CrossRef](#)]
18. Albatici, R.; Tonelli, A.M.; Chiogna, M. A comprehensive experimental approach for the validation of quantitative infrared thermography in the evaluation of building thermal transmittance. *Appl. Energy* **2015**, *141*, 218–228. [[CrossRef](#)]
19. Fokaides, P.A.; Kalogirou, S.A. Application of infrared thermography for the determination of the overall heat transfer coefficient (U-Value) in building envelopes. *Appl. Energy* **2011**, *88*, 4358–4365. [[CrossRef](#)]
20. Dall’O’, G.; Sarto, L.; Panza, A. Infrared screening of residential buildings for energy audit purposes: Results of a field test. *Energies* **2013**, *6*, 3859–3878. [[CrossRef](#)]
21. Nardi, I.; Sfarra, S.; Ambrosini, D. Quantitative thermography for the estimation of the U-value: state of the art and a case study. In Proceedings of the 32nd UIT (Italian Union of Thermo-fluid-dynamics) Heat Transfer Conference, Pisa, Italy, 23–25 June 2014.
22. Nardi, I.; Ambrosini, D.; Rubeis, T.D.; Sfarra, S.; Perilli, S.; Pasqualoni, G. A comparison between thermographic and flow-meter methods for the evaluation of thermal transmittance of different wall constructions. In Proceedings of the 33th UIT (Italian Union of Thermo-fluid-dynamics) Heat Transfer Conference, L’Aquila, Italy, 22–24 June 2015.
23. ISO 6946: 2007. Building Components and Building Elements—Thermal Resistance and Thermal Transmittance—Calculation Method. Available online: <https://www.iso.org/standard/40968.html> (accessed on 13 July 2017).
24. Simões, I.; Simões, N.; Tadeu, A.; Riachos, J. Laboratory assessment of thermal transmittance of homogeneous building elements using infrared thermography. In Proceedings of the 12th International Conference on Quantitative InfraRed Thermography, Bordeaux, France, 7–12 July 2014.
25. Rhee-Duverne, S.; Baker, P. Research into the Thermal Performance of Traditional Brick Walls. 2013. Available online: <https://content.historicengland.org.uk/images-books/publications/thermal-performance-traditional-windows-summary/sash-windows-research-summary.pdf/> (accessed on 30 June 2017).
26. DYNAMIC Analysis, Simulation and Testing Applied to the Energy and Environmental Performance of Buildings (DYNASTEE). Available online: <http://dynastee.info/data-analysis/software-tools/lord> (accessed on 30 June 2017).
27. LORD 3.2. Available online: <http://dynastee.info/wp-content/uploads/2012/12/lordmanual.pdf> (accessed on 30 June 2017).
28. Gutschker, O. Parameter identification with the software package LORD. *Build. Environ.* **2008**, *43*, 163–169. [[CrossRef](#)]
29. Madding, R. Finding R-values of stud frame constructed houses with IR thermography. In Proceedings of the InfraMation, Reno, NV, USA, 3–7 November 2008; pp. 261–277.
30. Watanabe, K. Architectural Planning Fundamentals, 1965.
31. ASTM C 680—14. Standard Practice for Estimate of the Heat Gain or Loss and the Surface Temperatures of Insulated Flat, Cylindrical, and Spherical Systems by Use of Computer Programs. Available online: <https://www.astm.org/Standards/C680.htm> (accessed on 13 July 2017).
32. Nardi, I.; Paoletti, D.; Ambrosini, D.; Rubeis, T.D.; Sfarra, S. U-value assessment by infrared thermography: A comparison of different calculation methods in a Guarded Hot Box. *Energy Build.* **2016**, *122*, 211–221. [[CrossRef](#)]
33. ASTM E 1862-97. Standard Test Methods for Measuring and Compensating for Reflected Temperature Using Infrared Imaging Radiometers. Available online: http://www.irss.ca/development/documents/CODES%20&%20STANDARDS_02-28-08/ASTM/Thermography/Test%20Method%20for/E1862-97%20Infrared%20Imaging%20Radiometers.pdf (accessed on 13 July 2017).
34. ASTM E 1933-99a. Standard Test Methods for Measuring and Compensating for Emissivity Using Infrared Imaging Radiometers. Available online: <https://www.astm.org/DATABASE.CART/HISTORICAL/E1933-99A.htm> (accessed on 13 July 2017).

35. Strachan, P.A.; Vandaele, L. Case studies of outdoor testing and analysis of building components. *Build. Environ.* **2008**, *43*, 129–142. [[CrossRef](#)]
36. Baker, P.H.; Dijk, H.A.L. PASLINK and dynamic outdoor testing of building components. *Build. Environ.* **2008**, *43*, 143–151. [[CrossRef](#)]



© 2017 by the authors. Licensee MDPI, Basel, Switzerland. This article is an open access article distributed under the terms and conditions of the Creative Commons Attribution (CC BY) license (<http://creativecommons.org/licenses/by/4.0/>).